# Promoting role of sulfur groups in selective catalytic reduction of NO with NH$_3$ over H$_2$SO$_4$ modified activated carbons

Qianqian Guo*,**, Wen Jing*,**, Shangzeng Cheng*,**, Zhanggen Huang*,†, Dekui Sun*,
Yaqin Hou*, and Xiaojin Han*

*State Key Laboratory of Coal Conversion, Institute of Coal Chemistry, Chinese Academy of Sciences,
Taiyuan 030001, P. R. China
**University of Chinese Academy of Sciences, Beijing 100049, P. R. China

**Abstract**−To determine the role of sulfur groups formed on activated carbon (AC) in the selective catalytic reduction (SCR) of NO with NH$_3$, coal-based AC was modified by H$_2$SO$_4$ under various conditions and then treated in N$_2$ atmosphere at 400 °C. The resulting carbons were characterized by N$_2$ adsorption, elemental analysis, temperature programmed desorption and X-ray photoelectron spectroscopy, and tested for the SCR of NO with NH$_3$ in the temperature range of 30-250 °C. Results reveal that H$_2$SO$_4$ modification has little effect on the textural properties, but promotes the formation of sulfur and oxygen groups. The sulfur groups incorporated by H$_2$SO$_4$ modification are mainly sulfonic groups and then sulfates. In particular, these sulfur groups play a predominant role in improving NH$_3$ adsorption and then enhancing the SCR activity of modified carbons above 150 °C. However, the contribution of oxygen groups to NO reduction is very limited under the conditions employed in this work.

Keywords: Activated Carbon, NO, H$_2$SO$_4$ Modification, Sulfur Groups, Oxygen Groups

## INTRODUCTION

NO is one of the main air pollutants due to its contribution to acid rain, photochemical smog and depletion of the stratospheric ozone layer [1,2]. The most effective technique to eliminate NO is the selective catalytic reduction (SCR) of NO with NH$_3$ [1,3-6].

The commercial SCR process uses V$_2$O$_5$/TiO$_2$ or V$_2$O$_5$-WO$_3$/TiO$_2$ as the catalytic system, which is located in the upstream of the desulfurizer and conducted in the temperature range of 300-400 °C [1,7]. However, the high concentrations of SO$_2$ and ash in flue gas reduce its catalytic activity and longevity. An attractive option to circumvent these problems is to place SCR unit in the downstream of the electrostatic precipitator and desulfurizer, where most of SO$_2$ and ash have been removed.

Activated carbon (AC) exhibits catalytic activity towards NO reduction with NH$_3$ at temperatures as low as 100-200 °C, making the SCR process easily retrofit into an existing flue gas cleaning system [4,8-10]. However, the main disadvantage of AC is the low SCR activity. Thus, modification of AC to improve its catalytic activity is necessary. In this case, one of the most investigated methods is the modification of AC by H$_2$SO$_4$ [4,5,8,9,11]. In previous studies, it was considered that H$_2$SO$_4$ modification introduced oxygen groups on carbon surface, which improved the adsorption of NH$_3$ and/or the oxidation of NO and thus enhanced the SCR activity [3-5,8,9]. However, the H$_2$SO$_4$ modification also results in the formation of sulfur groups, which play an important role in some re-

action processes, such as catalytic wet peroxide oxidation [12-14] and the adsorption of water vapor [15]. Despite these, little information is available on the role of sulfur groups in the promoted SCR activity. In this regard, two aspects including the nature of the sulfur groups and the way of these groups affecting the SCR process remain unclear.

In the present work, the coal-based AC was modified by H$_2$SO$_4$ under various conditions and then treated in N$_2$ atmosphere at 400 °C in order to obtain carbons with different chemical properties. The resulting carbons were characterized by N$_2$ adsorption, elemental analysis, temperature programmed desorption (TPD) and X-ray photoelectron spectroscopy (XPS), and tested for NO reduction with NH$_3$ in the temperature range of 30-250 °C. The objective of this work was to determine the role of sulfur groups incorporated by H$_2$SO$_4$ modification in the SCR of NO with NH$_3$.

## EXPERIMENTAL

### 1. Catalyst Preparation

The coal-based AC used in this study was purchased from Xinhua Chemical Plant, China. Prior to H$_2$SO$_4$ modification, the AC was crushed and sieved into 30-60 mesh particles. Then, 10 g of the AC was modified by 50 mL H$_2$SO$_4$ for 10 h, followed by washing with distilled water to remove the residual acid until neutrality of the rinsing water was reached, and then drying at 110 °C for 10 h. Some of the resulting carbons were calcined at 400 °C in N$_2$ atmosphere until no SO$_2$ was detected (less than 10 min). Table 1 summarizes the AC surface treatments and their designations.

### 2. Catalyst Characterization

The textural properties of the carbons were measured by N$_2$ ad-

**Table 1. Specification of the AC surface treatments**

| Notation | Surface treatment |
|----------|-------------------|
| AC | The original activated carbon |
| ACS1 | The AC modified by 2.5 mol/L $H_2SO_4$ at 30 $^\circ$C |
| ACS2 | The AC modified by 2.5 mol/L $H_2SO_4$ at 80 $^\circ$C |
| ACS3 | The AC modified by concentrated $H_2SO_4$ at 80 $^\circ$C |
| AC-400 | The AC calcined at 400 $^\circ$C in $N_2$ atmosphere |
| ACS1-400 | The ACS1 calcined at 400 $^\circ$C in $N_2$ atmosphere |
| ACS2-400 | The ACS2 calcined at 400 $^\circ$C in $N_2$ atmosphere |
| ACS3-400 | The ACS3 calcined at 400 $^\circ$C in $N_2$ atmosphere |

sorption isotherm at 77 K using a Micromeritics, ASAP2020 analyzer. Prior to measurement, the samples were degassed at 150 $^\circ$C for 10 h. Specific surface area was calculated by applying the Brunauer-Emmett-Teller (BET) equation. Micropore volume was obtained from the Dubinin-Radushkevich (DR) methods.

Elemental analysis of each sample was performed using a Vario EL from Elementar Analysensysteme GmbH.

TPD experiments were performed under 50 mL/min of Ar flow by heating the sample from room temperature to 1,000 $^\circ$C at a heating rate of 10 $^\circ$C/min. The evolution of CO, $CO_2$, and $SO_2$ as a result of the decomposition of oxygen and sulfur groups was monitored by a quadrupole mass spectrometer (OmniStar).

XPS was carried out on a KRATOS XSAM800 fitted with an Al $K\alpha$ source (1,486.6 eV). The anode was operated at 120 W and the analyzer was operated at constant narrow scan pass energy of 30 eV. The analysis area was 8 mm×8 mm. The photoelectrons were collected at an electron take off angle of 60$^\circ$. The binding energy shifts due to surface charge were corrected using the C1s core level at 284.8 eV as an internal standard.

**3. Activity Test**

A schematic diagram of the experimental apparatus is in Fig. 1. The activity test was in a fixed bed reactor (i.d. 10 mm) and 2 g of sample was used. The simulated flue gas consisted of 500 ppm NO,
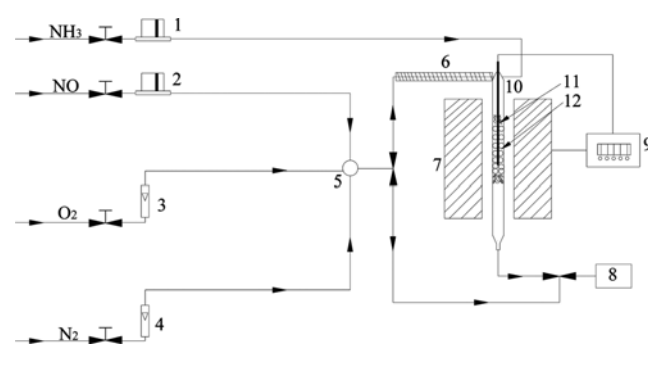
**Fig. 1. Schematic diagram of experimental apparatus for activity test.**

1, 2. Mass flow controller 　 9. Program temperature
3, 4. Rotameter 　　　　　　　　 controller
5. Mixing chamber 　　　　 10. Reactor
6. Preheater 　　　　　　　 11. Quartz wool
7. Furnace 　　　　　　　　 12. Catalyst
8. Flue gas analyzer

500 ppm $NH_3$, 4% $O_2$ and $N_2$ to balance. The total flow rate was maintained at 400 mL/min corresponding to the GHSV of 6,000 h$^{-1}$. In all runs, the test proceeded for 3 h at desired temperature to reach steady-state NO conversion. The outlet concentrations of NO and $O_2$ were measured online by a flue gas analyzer (KM9106 Quintox, Kane International Limited). In some cases, the outlet gases evolution was monitored by a Gasmet DX4000 FT-IR gas analyzer, and the concentrations of $N_2O$ were less than 5 ppm. The NO conversion is calculated as follows:

$$\text{Conversion (\%)} = \frac{C_{in} - C_{out}}{C_{in}} \times 100$$

where $C_{in}$ is the initial concentration of NO and $C_{out}$ corresponds to its concentration once steady state is reached.

**4. Adsorption of $NH_3$**

To estimate the affinity of $NH_3$ with carbon surface, the breakthrough behavior of $NH_3$ over carbons was investigated. 1 g of sample was loaded in the fixed bed reactor and exposed to gas mixture containing 500 ppm $NH_3$+4% $O_2$+$N_2$ at the flow rate of 400 mL/min. The outlet concentrations of $NH_3$ were continuously monitored by a JNYQ-I-41C $NH_3$ analyzer.

**RESULTS AND DISCUSSIONS**

**1. Physical Property**

The physical properties of carbons are listed in Table 2. The $H_2SO_4$ modification results in slight decreases in BET surface area and total pore volume compared with the AC, which is due to the collapse of pore walls and/or the formation of oxygen and sulfur groups located at the entrance of the pores to make the pore volume decrease [5,8,16,17]. Meanwhile, slight increases in micropore surface area and volume are observed. The reason for this is the widening of narrow micropore which makes them accessible to $N_2$ adsorption at 77 K [17]. Generally, the change in the BET surface area after $H_2SO_4$ modification is in line with the micropore area [16-18]. The slightly opposite trend of the two parameters shown in Table 2 reflects that the textural properties not only depend on the treatment conditions but also on the nature of activated carbons. Compared with carbons without calcination, the BET surface area and pore volume of the calcined carbons slightly increase, probably due to the decomposition of some oxygen and/or sulfur groups with less thermal stability.

Although the textural properties of carbons have been shown to

**Table 2. Surface area and pore volume of carbons**

| | $S_{BET}$ (m$^2$/g) | $S_{micro}$ (m$^2$/g) | $V_{total}$ (cm$^3$/g) | $V_{micro}$ (cm$^3$/g) |
|---|---|---|---|---|
| AC | 957 | 517 | 0.553 | 0.236 |
| ACS1 | 941 | 521 | 0.544 | 0.239 |
| ACS2 | 932 | 530 | 0.532 | 0.243 |
| ACS3 | 927 | 543 | 0.527 | 0.248 |
| AC-400 | 959 | 527 | 0.555 | 0.242 |
| ACS1-400 | 952 | 540 | 0.552 | 0.247 |
| ACS2-400 | 951 | 549 | 0.550 | 0.251 |
| ACS3-400 | 943 | 557 | 0.549 | 0.260 |

**Table 3. Chemical composition of carbons obtained by elemental analysis**

| | Elemental analysis (wt%) | | | | |
|---|---|---|---|---|---|
| | $C_{ad}$ | $H_{ad}$ | $O_{ad}$ | $N_{ad}$ | $S_{ad}$ |
| AC | 84.22 | 1.09 | 2.14 | 0.45 | 0.47 |
| ACS1 | 83.35 | 1.24 | 3.02 | 0.43 | 0.81 |
| ACS2 | 82.56 | 1.37 | 3.54 | 0.44 | 0.93 |
| ACS3 | 80.99 | 1.65 | 4.64 | 0.41 | 1.08 |
| AC-400 | 85.69 | 0.92 | 1.77 | 0.55 | 0.45 |
| ACS1-400 | 84.68 | 0.95 | 2.27 | 0.56 | 0.51 |
| ACS2-400 | 83.28 | 0.98 | 2.56 | 0.54 | 0.52 |
| ACS3-400 | 81.87 | 1.03 | 3.32 | 0.52 | 0.52 |

ad: air dry

affect the NO reduction with $NH_3$ [19], their performance will be considered to be minor in this work since the changes in pore structure caused by $H_2SO_4$ modification are unnoticeable.

**2. Surface Chemistry**

The chemical composition of carbons obtained by elemental analysis is shown in Table 3. In all cases, the major elements are carbon and oxygen. The $H_2SO_4$ modification results in increases in the oxygen and sulfur content, which increases with the degree of the modification conditions, indicating the formation of oxygen and sulfur groups [3,20]. After calcination at 400 °C in $N_2$ atmosphere, the oxygen content of all the carbons decreases. Additionally, the sulfur content of modified carbons after calcination is reduced to the comparable level with that of the AC-400. The decrease in sulfur content was undoubtedly attributed to the decomposition of sulfur groups, while the decreased oxygen content perhaps was attributed to the decomposition of oxygen groups in addition to that of sulfur groups. Regardless of the calcination, the oxygen content follows an order of AC<ACS1<ACS2<ACS3.

To determine the nature of sulfur and oxygen groups as a result of $H_2SO_4$ modification, TPD experiments were performed on carbons. The CO, $CO_2$ and $SO_2$ release profiles are shown in Fig. 2. As can be seen, the CO release profile of the original AC starts at about 800 °C, peaks at 930 °C and does not desorb completely up to 1,000 °C, which is due to the decomposition of carbonyl and/or pyrone type structures [21,22]. Compared with the original AC, the intensity of the peak at 930 °C on the modified carbons decreases, whereas a small peak at 265 °C appears. Such a phenomenon becomes more pronounced as the degree of the modification conditions increases.

In the case of $CO_2$, the AC shows a broad asymmetric $CO_2$ peak at 700 °C as a result of the decomposition of lactones existing in different chemical environments [21,23]. After $H_2SO_4$ modification, the intensity of this peak is enhanced, indicating the formation of lactone groups. Simultaneously, a new peak at 265 °C is also observed and its intensity increases with the extent of treatment. Additionally, after $H_2SO_4$ modification, an $SO_2$ release peak at 265 °C appears, the intensity of which also increases with the extent of treatment, while no $SO_2$ is released over the AC.

As a strong acid, it could be expected that the $H_2SO_4$ modification is favorable for the formation of acidic $CO_2$-type groups but
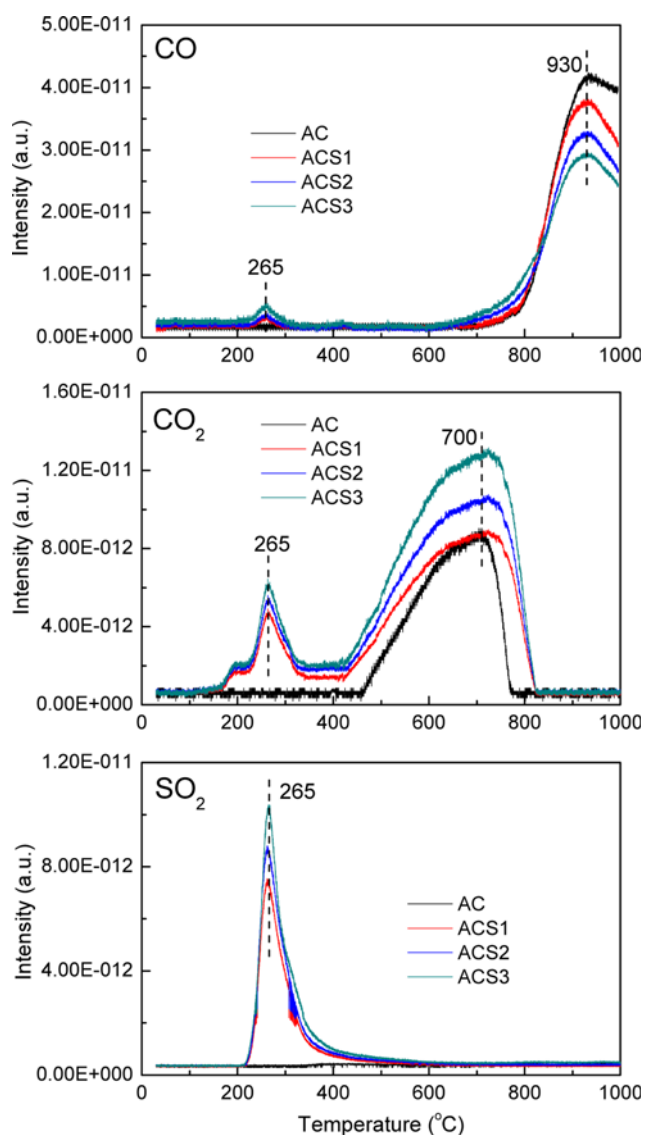


Fig. 2. The CO, $CO_2$, and $SO_2$ profiles during the TPD experiments.

inhibits that of carbonyl and pyrone type groups, thus leading to the evolution of lactone, carbonyl, and pyrone type groups with the degree of treatment conditions. The newly formed CO and $CO_2$ peak at 265 °C has two possible assignments: (i) the oxygen groups with less thermal stability; and (ii) the interaction between the sulfur groups and the carbon. However, the CO and $CO_2$ peak at 265 °C excellently corresponds to the $SO_2$ release peak (temperature and shape) over the modified carbons, which is attributed to the decomposition of thiols and oxidized sulfur groups [13,24,25], thus prompting us to assign this peak to the interaction between the sulfur groups and the carbon rather than the oxygen groups. In other words, the decomposition of thiols and oxidized sulfur groups and their interaction with the carbon lead to the formation of $SO_2$, CO, and $CO_2$ release peak at 265 °C. Additional information obtained from Fig. 2 is that the decomposition of lactone groups starts at temperatures much higher than 400 °C, implying that the decrease in the oxygen content after calcination at 400 °C (Table 2), is mainly because of the decomposition of the sulfur groups rather than the

oxygen groups.

As shown in Fig. 2, the $H_2SO_4$ modification does not introduce carboxyl, anhydride, and phenol groups on the coal-based AC under the conditions used in this work, which is different from previous reports [4,5,8]. Such a result is most likely attributed to the different nature of AC used in this work in comparison with other studies. Thus, only the sulfur groups are decomposed after the calcination in $N_2$ atmosphere at 400 °C. This result is useful to determine the role of sulfur groups in the SCR process, which will be discussed in detail below.

To get further insight into the nature of sulfur groups, some of the carbons were characterized by XPS. Deconvolution of S2p spectra is shown in Fig. 3. For the AC, the peaks located at 163.9 and 165.1

eV are assigned to the sulfur species on AC matrix. After $H_2SO_4$ modification (ACS2), the S2p spectrum indicative of sulfur species on AC is unchanged, but two new peaks appear. Moreover, the intensity of two new peaks is higher than that of the peaks at 163.9 and 165.1 eV, implying the formation of new sulfur groups acting as the main sulfur species on modified carbons. After calcination, the newly formed peaks disappear, while the other peaks assigned to the sulfur species on the AC are unchanged, indicating the decomposition of newly formed sulfur groups, consistent with the TPD results in Fig. 2.

Standard library spectra provide the following information about the peaks related to sulfur species: organic sulfur (-SH) has a peak around 164 eV [26]; elemental sulfur has a peak at about 165 eV
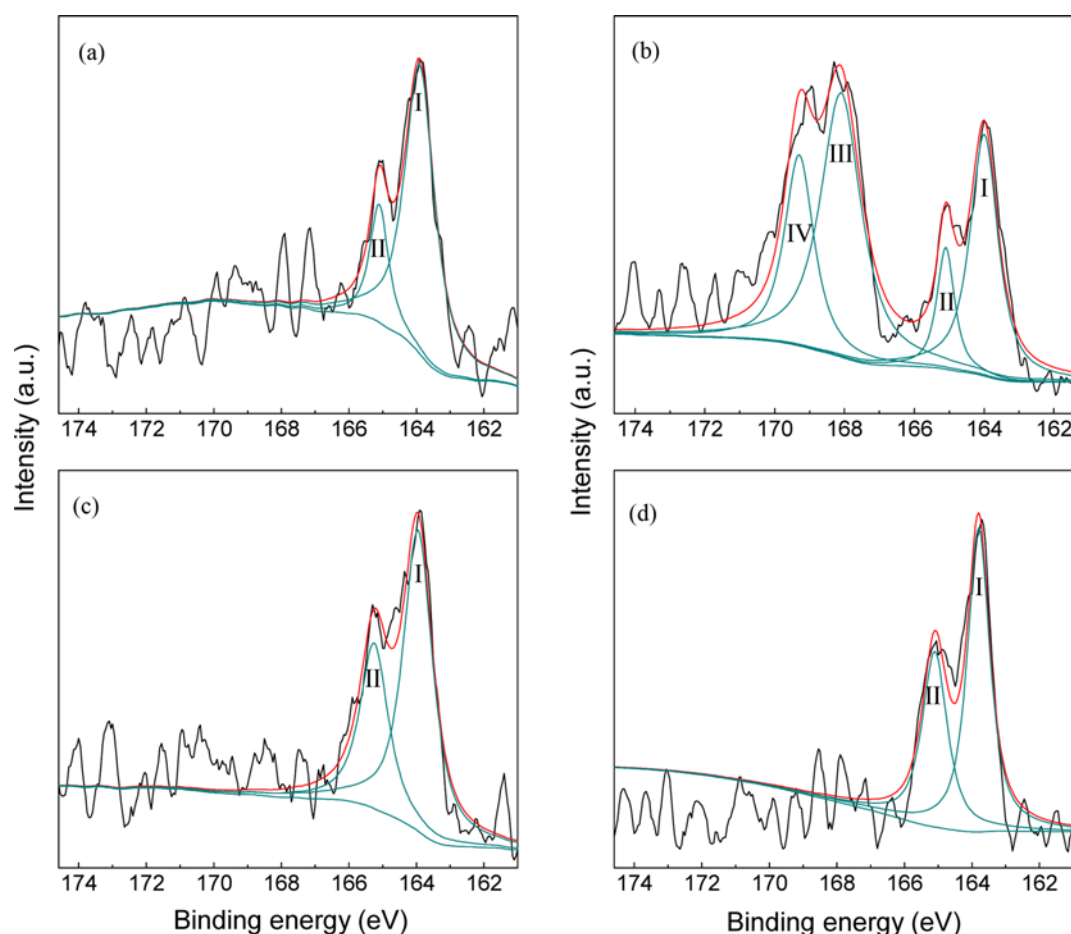


Fig. 3. Deconvolution of S2p spectra from XPS. (a) AC; (b) ACS2; (c) AC-400; and (d) ACS2-400.

Table 4. Concentration of sulfur components in S2p spectra of carbons

| | Peak I | | Peak II | | Peak III | | Peak IV | | Total[a] |
|---|---|---|---|---|---|---|---|---|---|
| | A[a] | Bm | A[a] | Bm | A[a] | Bm | A[a] | Bm | |
| AC | 0.46 | 163.9 | 0.14 | 165.1 | - | - | - | - | 0.60 |
| ACS2 | 0.35 | 164.0 | 0.11 | 165.1 | 0.56 | 168.1 | 0.29 | 169.3 | 1.31 |
| AC-400 | 0.34 | 163.9 | 0.18 | 165.2 | - | - | - | - | 0.52 |
| ACS2-400 | 0.37 | 163.8 | 0.20 | 165.1 | - | - | - | - | 0.57 |

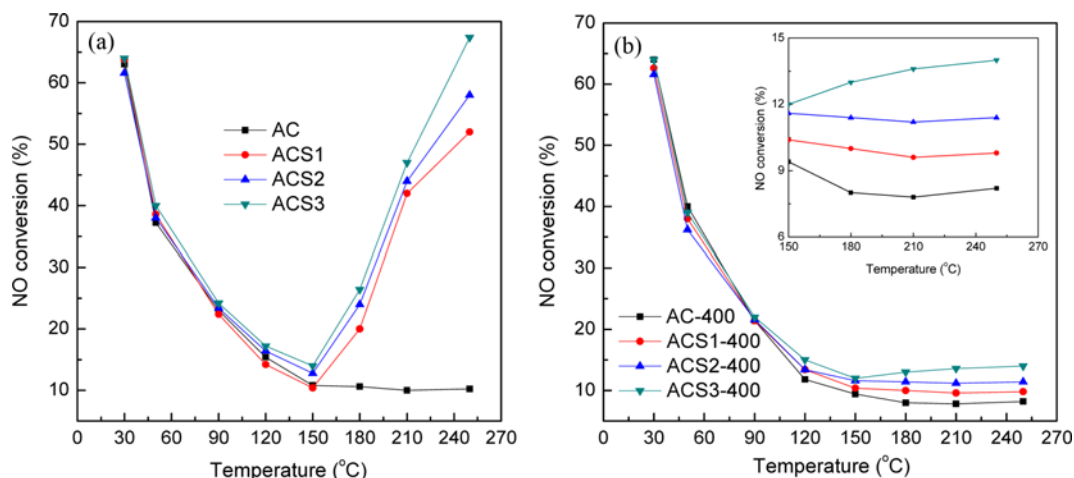[a]Amount of sulfur groups (wt%); Bm: the binding energy of peak maximum

**Fig. 4. Variation of NO conversion with temperature over carbons. Reaction conditions: 500 ppm NO, 500 ppm NH₃, 4% O₂, N₂ as balance, and GHSV of 6,000 h⁻¹.**

[20,26]; the oxidized sulfur groups, such as sulfonic groups and sulfates, have a peak above 167 eV [27,28]. Moreover, the binding energy of sulfates is higher than that of sulfonic groups. Accordingly, the four obvious maxima at 164.0, 165.1, 168.1, and 169.3 eV in ACS2 could be assigned to -SH, elemental sulfur, -SO₃H, and sulfate, respectively. To determine the amount of each sulfur species, the S2p spectra are fitted into the above-mentioned four peaks, and the results are shown in Table 4. It may be concluded that (i) the H₂SO₄ modification mainly introduces sulfonic groups and sulfates, the amount of the former being about twice that of the latter, and (ii) both the H₂SO₄ modification and the calcination have little effect on the amount of -SH and elemental sulfur.

According to the combined TPD and XPS results, it could be concluded that the sulfur groups formed after H₂SO₄ modification are mainly sulfonic groups and then sulfates.

**3. Activity Test**

Fig. 4 shows the temperature dependence of NO conversion over carbons. As shown in Fig. 4(a), the NO conversion over the AC continuously decreases from 63.0% to 10.8% when the temperature increases from 30 °C to 150 °C, with the value keeping stable above 150 °C. The H₂SO₄ modification has little effect on NO conversion at the temperatures lower than 150 °C, but significantly improves the activity above 150 °C, leading to the increased NO conversion with temperature in the range of 150-250 °C. The different temperature dependences of NO conversion over modified carbons before and after 150 °C indicate that two different mechanisms may be operative in this process [4,10,18]. According to previous study [4], the SCR reaction most likely takes place between adsorbed NO and adsorbed NH₃ at lower temperatures, following the L-H mechanism. In this case, the adsorption of reactants is the rate-determining step. Increasing temperature inhibits the adsorption of reactants, and thus results in the decreased NO conversion with temperature in the temperature range of 30-150 °C. Above 150 °C, the SCR reaction occurs between gaseous NO and adsorbed NH₃, following E-R mechanism. In this case, the activation of adsorbed NH₃ is the rate-determining step. Increasing temperature is favorable for NH₃ activation and thus leads to increased NO con-

version with temperature.

Since the change in textural properties after H₂SO₄ modification is not notable (see Table 2), the enhanced activity is attributed to the formation of sulfur and/or oxygen groups. Moreover, good tolerance of H₂SO₄ modified activated carbons to H₂O poison was found during the SCR process. In the case of the ACS2, addition of 2.5% H₂O into the feed resulted in a decrease of NO conversion from 58.0% to 46.0% within 20 min, but a further decrease was not observed within 3 h at 250 °C (not shown).

Additionally, calcination has little effect on the SCR activity of the AC, but significantly affects that of modified carbons. As illustrated in Fig. 4(b), the NO conversion continuously decreases with the increasing reaction temperature over the calcined carbons. The promoting effect of H₂SO₄ modification above 150 °C diminishes to a large extent after calcination. From TPD results (Fig. 2), apparently the sulfur groups, namely the sulfonic groups and sulfates, are decomposed after the calcination at 400 °C, while the oxygen groups remain stable. This strongly indicates that the decrease in NO conversion over the modified carbons above 150 °C after calcination is because of the decomposition of sulfur groups. The sulfonic groups and sulfates, rather than the oxygen groups, thus play a predominant role in the promoted NO conversion above 150 °C, as shown in Fig. 4(a).

In most cases the oxygen groups significantly enhance the SCR activity [4,5,8], which is not obvious in our case. This is because the promotion effect might depend on the amount as well as the nature of oxygen groups. On the one hand, as shown in Table 3 and Fig. 2, the amount of oxygen groups introduced by H₂SO₄ modification is relatively low. On the other hand, it has been reported that the carboxyl and phenol groups promote NH₃ adsorption [8], while the other oxygen groups might have relatively weak effect. The TPD results in Fig. 2 indicate that the main oxygen groups on carbons after H₂SO₄ modification are lactone, carbonyl and pyrone groups, rather than carboxyl and phenol groups.

To determine the role of sulfonic groups and sulfates during SCR reaction, the breakthrough behaviors of NO and NH₃ over carbons in the presence of oxygen were investigated. It was found that the
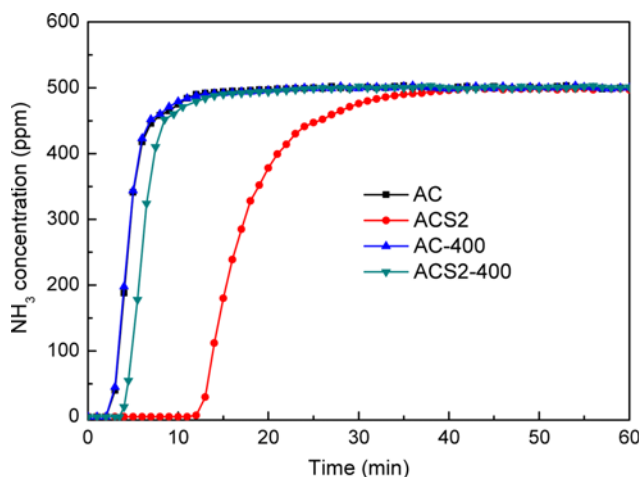
Fig. 5. The NH₃ breakthrough profiles over carbons at 30 °C. Reaction conditions: 500 ppm NH₃, 4% O₂, N₂ as balance, and GHSV of 12,000 h⁻¹.

breakthrough behavior of NO over modified carbons is similar to that over the AC (not shown), indicating that the $H_2SO_4$ modification has little effect on the adsorption and oxidation of NO. However, the $H_2SO_4$ modification significantly improves $NH_3$ adsorption. As shown in Fig. 5, the breakthrough of $NH_3$ over the AC occurs at 3 min, with its concentration increasing abruptly to the inlet value within 10 min. By contrast, the $NH_3$ breakthrough over the ACS2 occurs at 13 min, and the increasing rate of outlet $NH_3$ concentration after the breakthrough point is slower than that of the AC. The breakthrough behavior of $NH_3$ over AC-400 is similar to that over the AC, indicating that the calcination has little effect on $NH_3$ adsorption. Compared with the AC, the breakthrough time of ACS2-400 increases, but significantly lower than that of the ACS2.

The amount of adsorbed $NH_3$ under different reaction temperatures was obtained by integrating the breakthrough profiles (see Fig. 6). The amount of adsorbed $NH_3$ decreases with the increasing reaction temperature, reflecting the exothermic nature of ad-



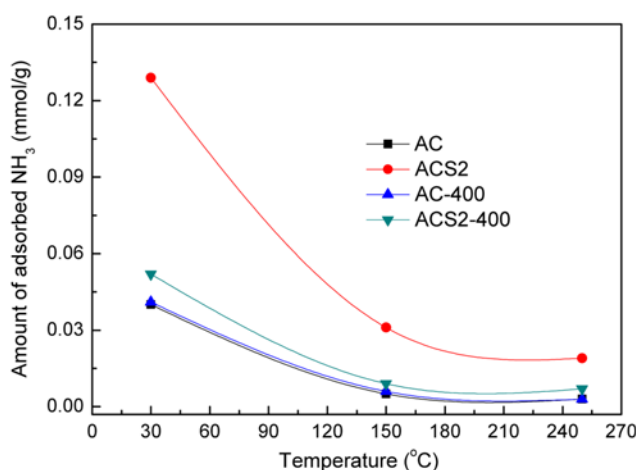Fig. 6. The amount of NH₃ adsorbed on carbons at various temperatures.

sorptive process. The $NH_3$ adsorbed on ACS2 is much higher than that on the other carbons, consistent with its promoted SCR activity above 150 °C. The lower amount of $NH_3$ adsorbed on ACS2-400 is most likely due to the decomposition of sulfur groups, since the oxygen groups keep stable after calcination at 400 °C. The sulfonic groups and sulfates, rather than the oxygen groups, thus play a predominant role in the $NH_3$ adsorption. The adsorbed $NH_3$ might be reactive towards NO reduction above 150 °C, and thus promotes SCR activity of modified carbons, as shown in Fig. 4(a). However, further studies are needed to reveal the nature of adsorbed $NH_3$ species and the NO reduction mechanism.

## CONCLUSIONS

Coal-based AC was modified by $H_2SO_4$ under various conditions and then treated in $N_2$ atmosphere at 400 °C. The resulting carbons were characterized by various techniques to determine the role of sulfur groups in the $NH_3$-SCR of NO. $H_2SO_4$ modification had little effect on the textural properties, whereas enhancing the sulfur and oxygen content. The TPD and XPS results revealed that the sulfur groups incorporated by $H_2SO_4$ modification are mainly sulfonic groups and then sulfates. These sulfur groups, as acidic sites, improve $NH_3$ adsorption. The adsorbed $NH_3$ is reactive towards NO reduction above 150 °C, and thus promotes the SCR activity of modified carbons. However, the oxygen groups have very limited contribution to NO reduction under the conditions employed in this work.

## ACKNOWLEDGEMENTS

## REFERENCES

1. G. Busca, L. Lietti, G. Ramis and F. Berti, *Appl. Catal. B: Environ.*, **18**, 1 (1998).
2. H. S. Zhu, Y. P. Mao, Y. Chen, X. L. Long and W. K. Yuan, *Korean J. Chem. Eng.*, **30**, 1241 (2013).
3. Z. Huang, Y. Hou, Z. Zhu and Z. Liu, *Catal. Commun.*, **50**, 83 (2014).
4. S. N. Ahmed, R. Baldwin, F. Derbyshire, B. McEnaney and J. Stencel, *Fuel*, **72**, 287 (1993).
5. A. Boyano, M. E. Gálvez, R. Moliner and M. J. Lázaro, *Fuel*, **87**, 2058 (2008).
6. L. Xiong, Q. Zhong, Q. Chen and S. Zhang, *Korean J. Chem. Eng.*, **30**, 836 (2013).
7. J. P. Chen and R. T. Yang, *J. Catal.*, **139**, 277 (1993).
8. H. Teng, Y. T. Tu, Y. C. Lai and C. C. Lin, *Carbon*, **39**, 575 (2001).
9. I. Mochida, M. Ogaki, H. Fujitsu, Y. Komatsubara and S. Ida, *Fuel*, **62**, 867 (1983).
10. M. E. Gálvez, M. J. Lázaro and R. Moliner, *Catal. Today*, **102-103**, 142 (2005).

11. A. Boyano, C. Herrera, M. A. Larrubia, L. J. Alemany, R. Moliner and M. J. Lázaro, *Chem. Eng. J.*, **160**, 623 (2010).

12. H. T. Gomes, S. M. Miranda, M. J. Sampaio, A. M. T. Silva and J. L. Faria, *Catal. Today*, **151**, 153 (2010).

13. H. T. Gomes, S. M. Miranda, M. J. Sampaio, J. L. Figueiredo, A. M. T. Silva and J. L. Faria, *Appl. Catal. B: Environ.*, **106**, 390 (2011).

14. R. P. Rocha, A. M. T. Silva, S. M. M. Romero, M. F. R. Pereira and J. L. Figueiredo, *Appl. Catal. B: Environ.*, **147**, 314 (2014).

15. J. Xiao, Z. L. Liu, K. Kim, Y. S. Chen, J. Yan, Z. Li and W. L. Wang, *J. Phys. Chem. C*, **117**, 23057 (2013).

16. Y. Xue, G. Lu, Y. Guo, Y. Guo, Y. Wang and Z. Zhang, *Appl. Catal. B: Environ.*, **79**, 262 (2008).

17. E. García-Bordejé, M. J. Lázaro, R. Moliner, P. M. Álvarez, V. Gómez-Serrano and J. L. G. Fierro, *Carbon*, **44**, 407 (2006).

18. M. C. Huang and H. Teng, *Carbon*, **41**, 951 (2003).

19. H. Teng, Y. F. Hsu and Y. T. Tu, *Appl. Catal. B: Environ.*, **20**, 145 (1999).

20. M. Mullett, P. Pendleton and A. Badalyan, *Chem. Eng. J.*, **211-212**, 133 (2012).

21. G. S. Szymański, Z. Karpiński, S. Biniak and A. Świątkowski, *Carbon*, **40**, 2627 (2002).

22. J. H. Zhou, Z. J. Sui, J. Zhu, P. Li, D. Chen, Y. C. Dai and W. K. Yuan, *Carbon*, **45**, 785 (2007).

23. J. L. Figueiredo, M. F. R. Pereira, M. M. A. Freitas and J. J. M. Órfão, *Carbon*, **37**, 1379 (1999).

24. A. P. Terzyk, *J. Colloid Interface Sci.*, **268**, 301 (2003).

25. S. Morales-Torres, T. L. S. Silva, L. M. Pastrana-Martinez, A. Brandao, J. L. Figueiredo and A. M. T. Silva, *Phys. Chem. Chem. Phys.*, **16**, 12237 (2014).

26. Z. Abdelouahab-Reddam, A. Wahby, R. El Mail, J. Silvestre-Albero, F. Rodriguez-Reinoso and A. Sepulveda-Escribano, *Adsorpt. Sci. Technol.*, **32**, 101 (2014).

27. G. Domazetis, M. Raoarun, B. D. James, J. Liesegang, P. J. Pigram, N. Brack and R. Glaisher, *Energy Fuels*, **20**, 1556 (2006).

28. M. Descostes, F. Mercier, N. Thromat, C. Beaucaire and M. Gautier-Soyer, *Appl. Surf. Sci.*, **165**, 288 (2000).